Open Access Journal

Journal of Power Technologies 98 (3) (2018) 245–254

journal homepage:papers.itc.pw.edu.pl

Forecast of global solar irradiation with a perfect model according to incline angle

Foued Chabane[a,b,*], Mohamed Amine Ghedhifi[a], Djamel Bensahal[c], Abdelhafid Bima[a,b], Noureddine Moummi[a,b]

[a] *Department of Mechanical Engineering, Faculty of Technology, University of Biskra 07000, Algeria;*
[b] *Mechanical Engineering Laboratory (LGM), Faculty of Technology, University of Biskra 07000, Algeria;*
[c] *Laboratory of Mechanics, Faculty of Technology, University of Laghouat, Algeria*

Abstract

The purpose of this study is to find and develop a model for measuring global solar irradiation at various angles from 0° to 90°. Through empirical studies, a suitable model for the studied site at Ouled Djellal, Biskra (Algeria) was developed, with preliminary data to be used in thermal simulation software for building and simulation of solar energy systems. The results of the proposed model were compared with the experimental data and there was excellent correlation.

Keywords: experimental study; solar irradiation; tilt angles; predicted model

1. Introduction

Solar energy occupies one of the most important places among the various possible alternative energy sources. An accurate knowledge of solar radiation distribution at a particular geographical location is of vital importance for the development of many solar energy devices and for creating performance estimates. Unfortunately, for many developing countries solar radiation measurements are not easily available, because they are unable to afford the cost of the measurement equipment and techniques involved. Therefore, it is important to elaborate methods to estimate the solar radiation on the basis of more readily meteorological data. Over the years, many models have been proposed to predict the amount of solar radiation, using various parameters. Some works used sunshine duration, others used mean daytime cloud cover or relative humidity and maximum and minimum temperature, while others still used the number of rainy days, sunshine hours and a factor that depends on latitude and altitude. Algeria is a high insolation country.

The use of simulation models is practically the only way to evaluate the evolution of solar radiation. Hard data are not always available, especially as solar radiation is measured at a limited number of sites around the world. To characterize a site, it is necessary to combine different types of models. The main models that are used to describe the solar field can be classified into three essential classes: empirical models, analytical models and stochastic models.

Different approaches and methods of estimating the solar field have been developed. Studies have been carried out to evaluate its spatial and temporal distribution during the year, the month, the day and the hour. The most common studies concern the modeling of solar radiation in different time scales and by different approaches. The physical or analytical methods are more complex than the theoretical models. They are elaborated from exact knowledge of the physical phenomena and allow researchers to calculate the transmission of solar radiation through the various layers of the atmosphere as precisely as possible. A precise description of the constituents of the atmosphere is needed to arrive at these models. Out-of-atmosphere irradiation is described by precise analytical expressions; the irradiation received on the ground is dependent on cloud cover and other atmospheric parameters. This gives it a randomness, hence the need to use more complex models.

Scientists deconstruct the atmosphere into horizontal layers and study successively the absorption and diffusion phenomena to which solar radiation is subjected. Other models give solar radiation according to atmospheric and astronomical parameters. Some examples of these models are:

In 1975, Perrin de Brichambaut [1] presented a model as a function of solar height and the atmospheric disturbance factor for estimating the daily average of the irradiation received on a horizontal plane by clear sky. Linke's disorder factor is defined for a pure, dry atmosphere (without aerosols, water vapor, or clouds).

Cole-Barbaro and al. [2] extend the Leone model to the calculation of direct, diffuse and global irradiation by any sky (generally cloudy) in terms of measurable parameters: the thickness of hot water condensable (w), sunshine by the relation S/So, the aerosol concentration (d) and nebulosity (Ne). They calculate the direct daily irradiation by a clear sky by

*Corresponding author
Email address: fouedmeca@hotmail.fr (Foued Chabane)

integrating the total direct flux (Leone's expression) between rising and setting.
In 1987, Capderou [2] proposed a model that uses the atmospheric cloud factor to calculate the direct and diffuse components of the irradiation received on a plane. The absorption and diffusion caused by the constituents of the atmosphere can be expressed by factors of disorder. From these factors, we can express the direct and diffused irradiations by clear sky.
The Kasten model [3] uses only total nebulosity, not information regarding the cloud layers. The coefficients used in the model were calculated from the measured data.
In 1960, Liu and Jordan [4] carried out monthly averages and after observing that statically the daily radiation is symmetrical in relation to the solar noon, they presented the results of their work in the form of abacuses, which various authors have proved as to validity in many countries including the United States, Canada, Australia and India. In recent decades, interest has been accentuated; several theoretical and experimental studies have taken place

Antonio Dumas & al. [5] reported that results in the monthly averaged daily values show a comparable accuracy with some well-recognized models such as the Angstrom–Prescott model, at least for the Mediterranean climatic area. They found that a high degree of accuracy can actually be achieved with both Dumas relationships. Jin-Ki Park & al. [6] developed an empirical model to estimate solar radiation from sunshine duration data over South Korea. They applied modeled data to a topographical factor at more than 50% of the area in South Korea. The Angstrom-Prescott-Page correlation has been subject to many modifications, either through modification of the Angstrom coefficients a and b [7, 8] or through the modification of the model itself [9, 10] that the Angstrom Prescott type correlations have been developed in many countries, including Austria [11], Belgium [12], Brazil [13], China [14], Czech Republic [11], India [15], Japan [16], Nigeria [17], North America [12], Oman [18], Saudi Arabia [19], Spain [9, 20], Turkey [21] and the UK [22].
Some researchers used solar irradiation as the source energy of the solar collector. It can therefore be concluded that solar irradiation has a great effect on the thermal efficiency of solar collectors [23, 24, 25, 26, 27, 28, 29, 30, 31, 32].

2. Fundamental Astronomy

Declination of the sun δ

Solar declination is the angle formed by the normal to the elliptical plane and the axis of rotation of the earth. It can also be defined as the angle between the center line of the sun-center of the earth and its projection on the equatorial plane of the earth. Its expression is given by:

$$\delta = 23.45 \sin\left[\frac{360}{365}(284 + n)\right]$$

where: n—the number of days of the year since 1 January.

Hour angle ω

The hour angle, h, of a point on the earth's surface is defined as the angle through which the earth would turn to bring the meridian of the point directly under the sun. The hour angle can also be obtained from the apparent solar time (AST); i.e., the corrected local solar time is :

$$\omega = (AST - 12) \times 15$$

The sun's altitude

The sun's altitude and azimuth angles can be determined in terms of the hour angle, declination angle, and latitude angle by the following formulas:

$$\sin h = \sin\delta \sin\varphi + \cos\delta \cos\varphi \cos\omega$$

$$a = \frac{\sin h \sin\varphi - \sin\delta}{\cos h \cos\varphi}$$

Height of the sun h

The Height angle (used interchangeably with altitude angle) is the angular height of the sun in the sky measured from the horizontal. Confusingly, both altitude and elevation are also used to describe the height in meters above sea level. The elevation is 0° at sunrise and 90° when the sun is directly overhead (which occurs for example at the equator on the spring and fall equinoxes).
The expression of h is as follows:

$$\sin h = \sin\delta \sin\varphi + \cos\delta \cos\varphi \cos\omega$$

$$h = \arcsin\left[\sin\delta \sin\varphi + \cos\delta \cos\varphi \cos\omega\right]$$

Angle of incidence θ

The angle of incidence is the angle formed between the direct solar radiation and the normal to the sensor inclined with respect to the horizontal plane by an angle i. For a sensor oriented towards the south, Incidence can be deduced:

$$\cos\theta = \cos(\varphi - i) \cos\delta \cos\omega + \sin(\varphi - i) \sin\delta$$

If the capture is not oriented, south θ can be found from h, α analytically:

$$\cos\theta = \cos h \cos(a - \gamma) \sin i + \sin h \cos i$$

In winter $i = \varphi + 10°$;
In summer $i = \varphi - 10°$.
i represent the angle of inclination and γ—the orientation in relation to the direction of the south.

Proposed model

The Sine wave function gives a good match with the experimental values (Fig. 1) and that is by oscillating around specified values. And it is formed with 4 parameters:

$$G = y_0 + A \times \sin\left(\pi\left(\frac{\frac{\omega}{h} - x_c}{\chi}\right)\right)$$

where: y_0—offset, A—amplitude, χ—period, x_c—phase shift, x—the division of $\frac{\omega}{h}$, ω—hour angle, h—height of the sun.

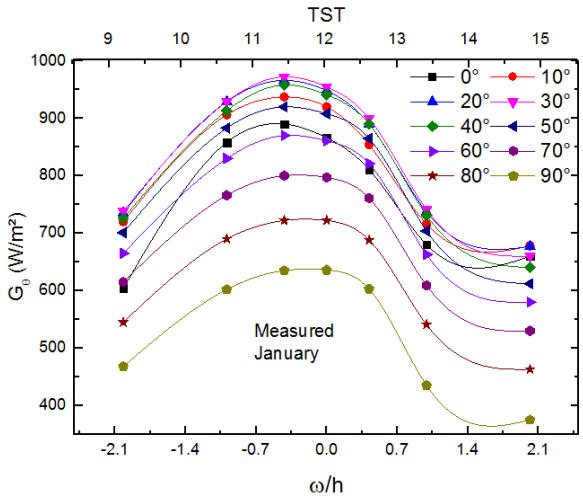

Figure 1: Comparison between experimental and the model proposed results

Table 1: Parameter values in January

β, °	January				
	y_0	x_c	χ	A	R^2
0	758.87	2.51	1.92	145.99	0.95797
10	803.80	2.77	2.16	142.5703	0.98783
20	820.99	2.89	2.23	153.6793	0.98437
30	817.63	3.02	2.31	161.441	0.98176
40	801.17	3.11	2.36	162.8851	0.98061
50	770.26	3.17	2.40	159.5614	0.97311
60	729.00	3.16	2.39	150.0034	0.96333
70	670.22	3.21	2.42	141.0528	0.95337
80	598.20	3.24	2.44	135.8782	0.95053
90	510.82	1.68	2.43	137.8253	0.90823

3. Experimental setup

The location of study is Ouled Djellal, approximately 400 kilometers south-east of Algiers. It is characterized in terms of the nature of the climate. We studied variations in temperature, humidity and wind power over a period of time in order to accurately identify the characteristics of the region and integrate them into our calculations for more accurate results. The equipment and mode of work are described below.

Geographic location [20]

Ouled Djellal is a district in Biskra Province in Algeria, about 100 km south-west of the city of Biskra (Fig. 2). Its geographical coordinates are: elevation 196 m above the sea, latitude 34° 26' 48.06" N and longitude 5° 6' 5.481" E.

Table 2: Parameter values in February

β, °	February				
	y_0	x_c	χ	A	R^2
0	599.99	3.13	2.25	190.9743	0.95503
10	647.30	-1.38	2.27	207.3004	0.96211
20	694.14	-1.31	2.13	224.2086	0.95146
30	699.55	-1.38	2.26	230.2606	0.97394
40	702.05	-1.39	2.25	236.2801	0.97968
50	691.21	-1.39	2.26	236.5582	0.98308
60	665.17	-1.41	2.26	235.4275	0.98524
70	626.21	3.09	2.26	228.915	0.9875
80	576.62	3.16	2.32	217.5184	0.99048
90	516.85	3.21	2.380	200.8242	0.98712

Table 3: Parameter values in March

β, °	March				
	y_0	x_c	χ	A	R^2
0	564.29	-1.65	2.59	302.74	0.7900
10	603.76	-1.66	2.57	317.31	0.7851
20	631.81	-1.67	2.57	334.09	0.79023
30	647.89	-1.68	2.56	339.11	0.7878
40	655.11	-1.68	2.55	346.47	0.79709
50	649.9365	-1.69	2.55	342.86	0.7949
60	630.0578	-1.69	2.55	335.64	0.79012
70	598.0371	-1.69	2.55	318.69	0.79469
80	552.9715	-1.70	2.5	287.55	0.80639
90	493.2105	-1.69	2.57	263.27	0.81601

Table 4: Parameter values in April

β, °	April				
	y_0	x_c	χ	A	R^2
0	708.13	6.06	4.49	204.26	0.99467
10	722.94	6.26	4.58	214.73	0.99476
20	722.26	6.34	4.59	231.69	0.99559
30	707.97	6.39	4.60	246.93	0.99775
40	687.17	6.59	4.69	247.57	0.99709
50	650.05	6.77	4.77	248.62	0.99578
60	595.06	6.79	4.78	254.76	0.9963
70	531.34	7.21	4.96	248.41	0.99395
80	458.37	7.52	5.10	230.74	0.98877
90	368.04	7.68	5.15	208.25	0.98514

3.1. Instrumentation and equipment used

Pyranometer

The solar radiation spectrum that reaches the earth's surface ranges from approximately 300 nm to 2800 nm. Depending on the type of pyranometer (Fig. 3) used, irradiance measurements with different degrees of spectral sensitivity will be obtained. To make a measurement of irradiance, it is required by definition that the response to "beam" radiation varies with the cosine of the angle of incidence. This ensures a full response when the solar radiation hits the sensor perpendicularly (normal to the surface, sun at zenith, 0° angle of incidence), zero response when the sun is at the horizon (90° angle of incidence, 90° zenith angle), and 0.5 at a 60° angle of incidence. It follows that a pyranometer should have a so-called "directional response" or "cosine response" close to the ideal cosine characteristic.

Table 5: Parameter values on a cloudy day

β, °	Cloudy day				
	y_0	x_c	χ	A	R^2
0	236.76	-0.95	1.25	190.65	0.76058
10	259.51	-1.02	1.29	217.61	0.83921
20	268.73	-1.05	1.31	230.16	0.75052
30	241.36	1.59	1.36	199.61	0.9686
40	240.87	1.59	1.37	195.24	0.95933
50	262.57	-1.11	1.39	215.31	0.75482
60	248.61	-1.09	1.37	206.33	0.7839
70	231.34	-1.06	1.35	190.59	0.76926
80	220.23	-1.09	1.38	182.16	0.78057
90	208.50	1.65	1.38	175.38	0.80429

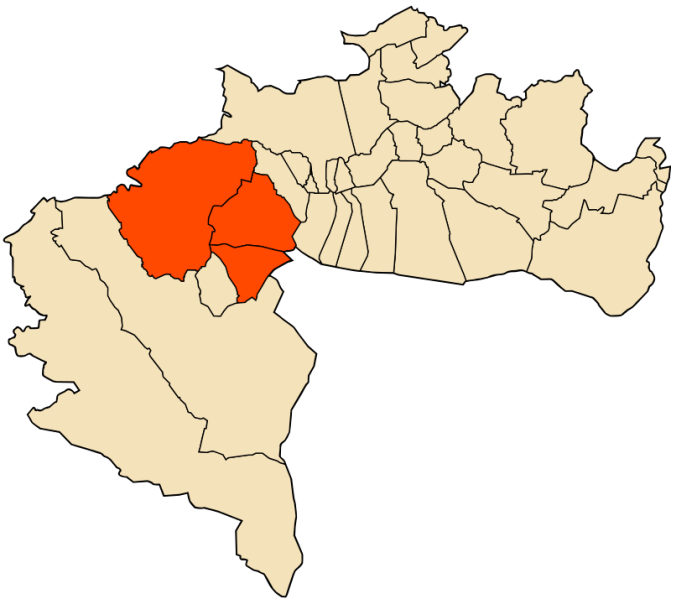

Figure 2: Location of Ouled Djellal in Biskra Province

Figure 3: The pyranometer

Compass

The compass (Fig. 4) has the important role of determining south. When the device is set in the direction of south the sun can be reeived permanently from sunrise to sunset.

Multi angled holder

Designed to carry the pyranometer and move in different angles this tool enables the operator to calculate the solar radiation with multiple angles. It comprises two rectangular panel bases made of wood, the principal base (28x14x3.5) cm, two metallic supports (8x4) cm fixed in the middle of it and an axis fixed at the extremity of the supports (Fig. 5). The axis is fixed on the center of the secondary base, which allows it to maneuver in a semicircular orbit a thin plank (40x14x0.3) cm affixed to the surface of the secondary base in order to obscure the effects of the other parts. A plastic protractor graduated from 0° to 90° is attached on the metallic support and an indicator is fixed on the axis so as to rotate with the panel.

Figure 4: The compass

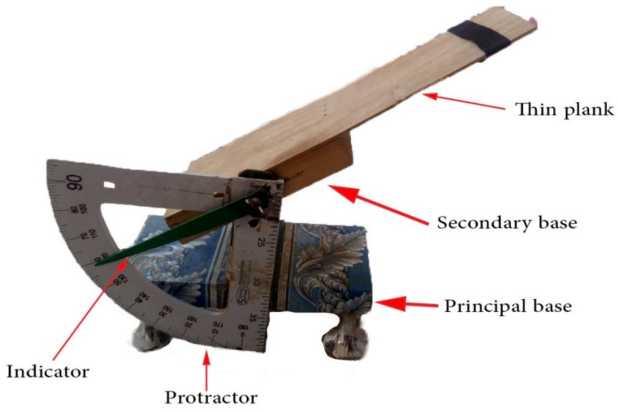

Figure 5: The multi angled holder

Knowledge of the site characterization and climate improves the study of global solar radiation determination. The various devices play an important role in determining global solar irradiation accurately.

4. Results

The experiments were carried out on tilt angles from 0° to 90° during the period January 2017 through April 2017. The tests were performed at Ouled Djellal (34° 26' 48.06" N and 5° 6' 5.481" E) in sunny and clear sky conditions and cloudy day conditions to test the model.

Figs. 6 and 7 show global irradiation as a function of the ratio of the hour angle and the height of the sun (ω/h) according to the tilt angles corresponding to experimental data in January. Maximum solar irradiation is in the tilt angle range of 20° through 40°, and the minimum is clearly at the angle $\theta = 90°$. Solar irradiation reaches its maximum at 11h30; $\theta = 30°$; $G_{30} = 972$ W/m^2 and its minimum is 390 W/m^2 at 15:00; $\theta = 90°$.

Fig. 8 shows global irradiation as a function of the ratio of the hour angle and the height of the sun (ω/h) according to the tilt angles corresponding to prediction data for January. The maximum solar irradiation is in the angle range from 20° to 40°, and the minimum corresponding to $\theta = 90°$. At 11h30

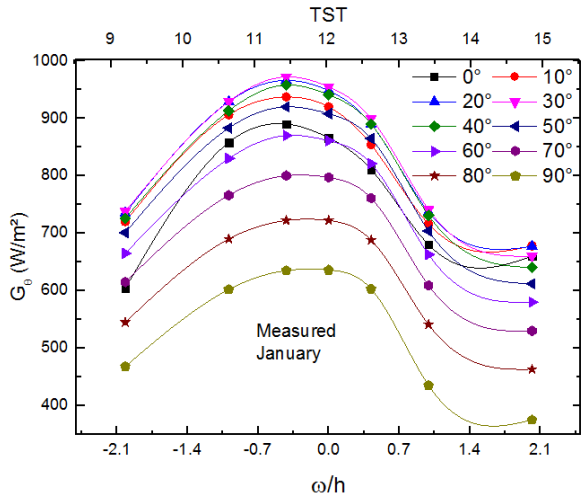

Figure 6: Global irradiation according to tilt angles and ω/h corresponding to experimental data in January

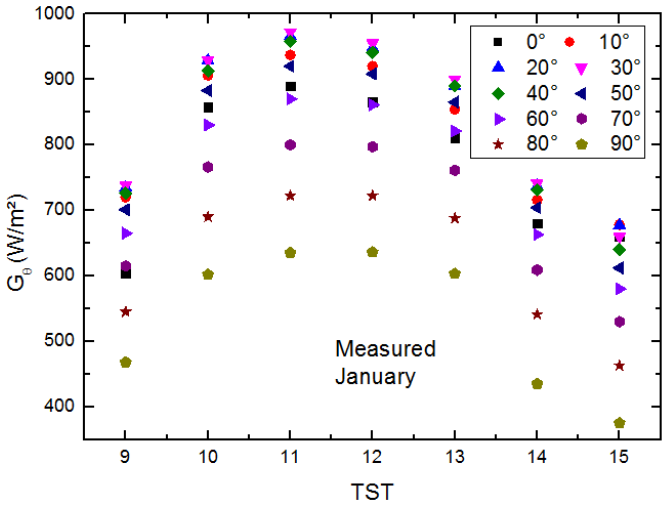

Figure 7: Global irradiation according to tilt angles and TST corresponding to experimental data in January

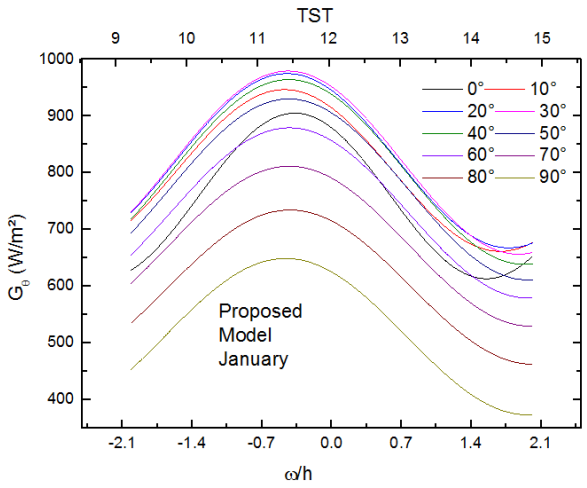

Figure 8: Global irradiation according to tilt angles corresponding to the proposed model in January

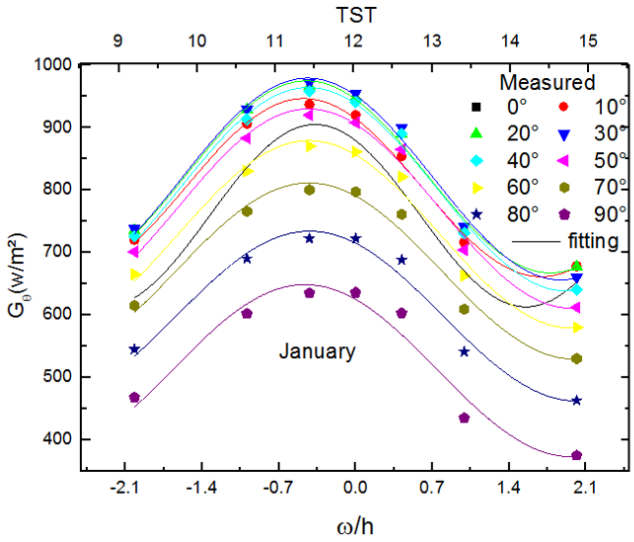

Figure 9: Comparison of global irradiation according to tilt angles between the proposed model and experimental data in January

solar irradiation reaches its maximum: $G_{30} = 972$ W/m^2 and its minimum is 390 W/m^2 at 15:00, $\theta = 90°$.

Fig. 9 compares global irradiation according to tilt angles between the proposed model and experimental data in January. As is presented in the given graphs the proposed model shows an almost identical match with the experimental data.

Figs. 10 and 11 show global irradiation as a function of the ratio of the hour angle and the height of the sun (ω/h) according to the tilt angles corresponding to experimental data in February. The maximum solar irradiation is in the tilt angle range from 30° to 50°, and the minimum is clearly at the angle $\theta = 90°$. Solar irradiation reaches its maximum at 11h30; $\theta = 40°$; $G_{30} = 955$ W/m^2 and its minimum is 730 W/m^2 at 12:00; $\theta = 90°$.

Fig. 12 shows global irradiation as a function of the ratio of the hour angle and the height of the sun (ω/h) according to the tilt angles corresponding to prediction data for February. The maximum solar irradiation is in the angle range from 20° to 40°, and the minimum corresponding to $\theta = 90°$. At 12h00 solar irradiation reaches its maximum; $G_{40} = 940$ W/m^2 and its minimum is 710 W/m^2 at 12:00; $\theta = 90°$.

Fig. 13 compares global irradiation according to tilt angles between the proposed model and experimental data in February. As is seen from the given graphs, the line of the proposed model crosses almost all the points of the experimental data.

Figs. 14 and 15 show global irradiation as a function of the ratio of the hour angle and the height of the sun (ω/h) according to the tilt angles corresponding to experimental data in March. Maximum solar irradiation is in the tilt angle range from 30° to 50°, and the minimum is clearly at the angle $\theta = 90°$. Solar irradiation reaches its maximum at 11h30;

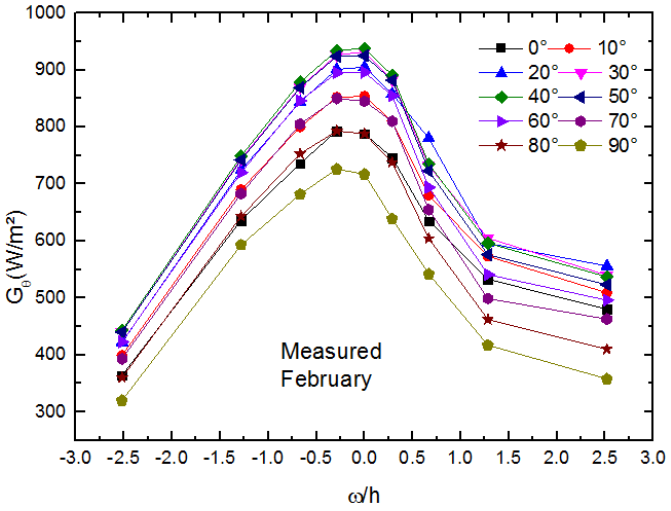

Figure 10: Global irradiation according to tilt angles and ω/h corresponding to experimental data in February

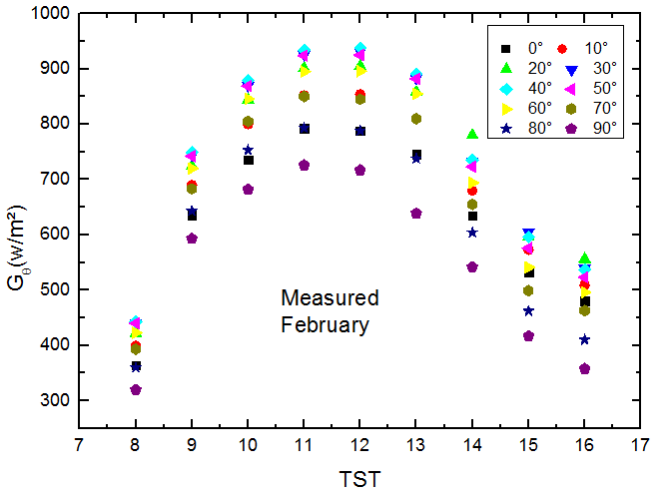

Figure 11: Global irradiation according to tilt angles and TST corresponding to experimental data in February

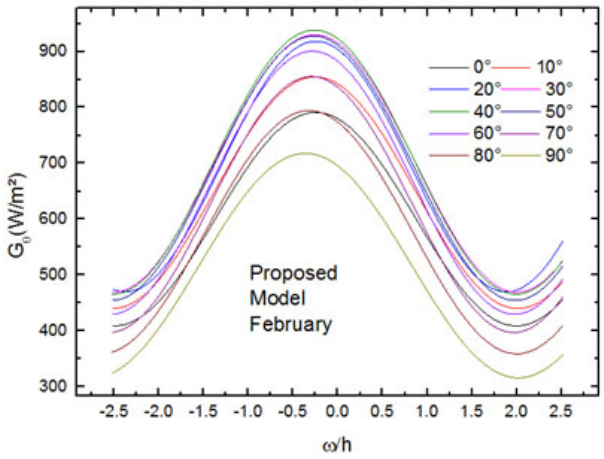

Figure 12: Global irradiation according to tilt angles corresponding to proposed model in February

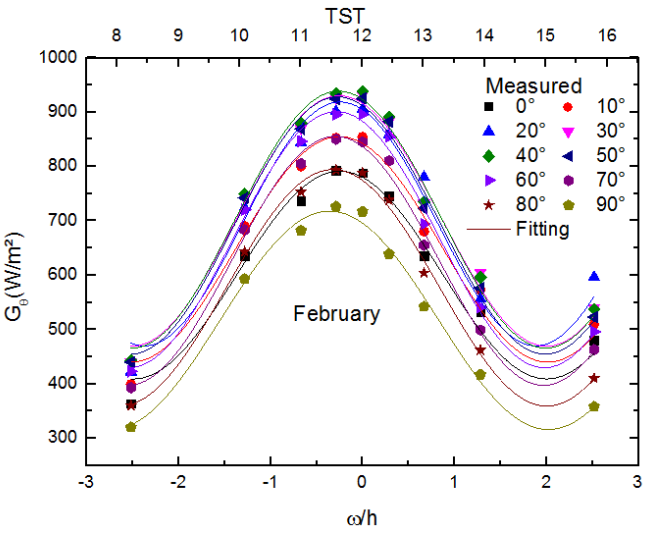

Figure 13: Comparison of global irradiation according to tilt angles between model and experimental data in February

$\theta = 40°$; $G_{40} = 1010$ W/m^2 and its minimum is 730 W/m^2 at 12:00; $\theta = 90°$.

Fig. 16 shows global irradiation as a function of the ratio of hour angle and the height of the sun (ω/h) according to the tilt angles corresponding to prediction data for March. The maximum solar irradiation is in the angle range from 30° to 50°, and the minimum corresponding to $\theta = 90°$. At 11h30 solar irradiation reaches its maximum; $G_{40} = 995$ W/m^2 and its minimum is 732 W/m^2 at 11:30; $\theta = 90°$.

Fig. 17 compares global irradiation according to tilt angles between the proposed model and experimental data in March. As is seen from the given graphs the line of the proposed model is a good match with the experimental data at $\omega/h = -3.9$, 0.5 and 1.

Figs. 18 and 19 show global irradiation as a function of the ratio of the hour angle and the height of the sun (ω/h) according to the tilt angles corresponding to experimental data in April. The maximum solar irradiation is in the tilt angle range from 20° to 40°, and the minimum is clearly at the angle $\theta = 90°$. The solar irradiation reaches its maximum at 11h30; $\theta = 20°$; $G_{20} = 980$ W/m^2 and its minimum is 560 W/m^2 at 12:00; $\theta = 90°$.

Fig. 20 shows global irradiation as a function of the ratio of the hour angle and the height of the sun (ω/h) according to the tilt angles corresponding to prediction data for April. The maximum solar irradiation is in the angle range from 20° to 40°, and the minimum corresponding to $\theta = 90°$. At 11h30 the solar irradiation reaches its maximum; $G_{30} = 975$ W/m^2 and its minimum is 550 W/m^2 at 15:00; $\theta = 90°$.

Fig. 21 compares global irradiation according to tilt angles between the proposed model and experimental data in April. As is seen from the given graphs the line of the proposed model crosses almost all the points of the experimental data.

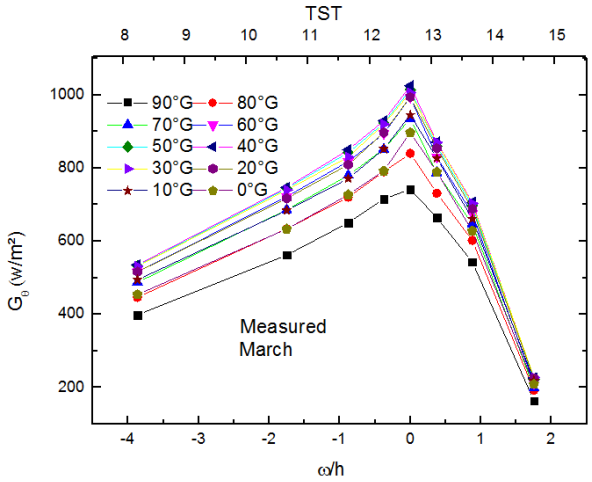

Figure 14: Global irradiation according to tilt angles and ω/h corresponding to experimental data in March

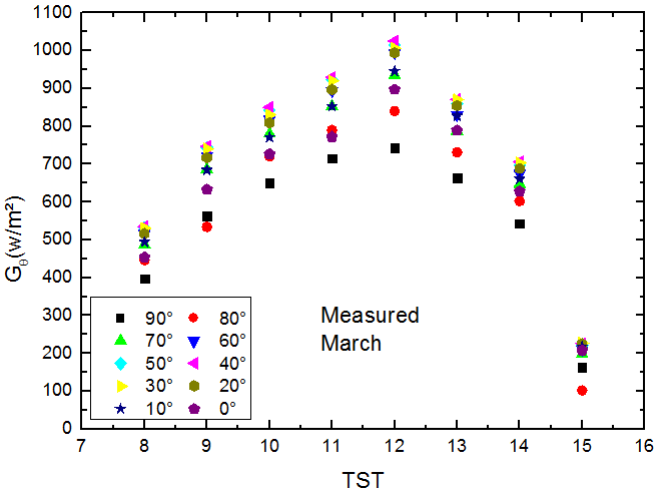

Figure 15: Global irradiation according to tilt angles and TST corresponding to experimental data in March

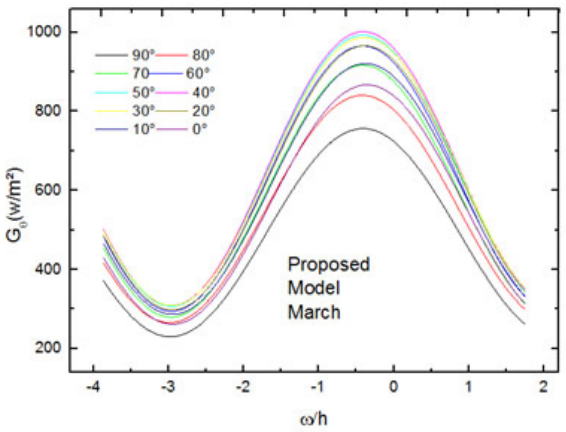

Figure 16: Global irradiation according to tilt angles corresponding to proposed model in March

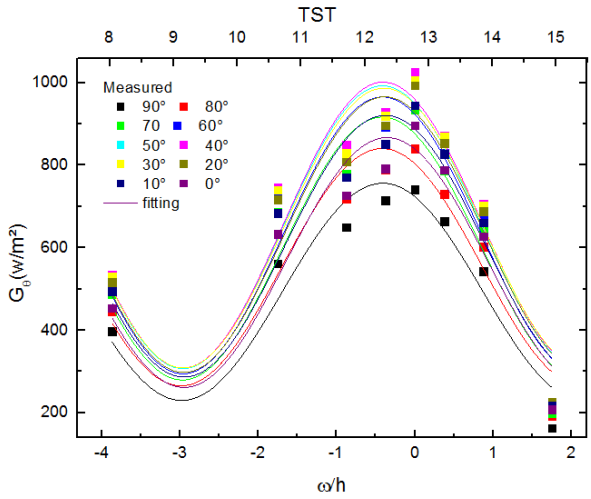

Figure 17: Comparison of global irradiation according to tilt angles between model and experimental data in March

Figs. 22 and 23 show global irradiation as a function of the ratio of the hour angle and the height of the sun (ω/h) according to the tilt angles corresponding to experimental data on a cloudy day. The maximum solar irradiation is in the tilt angle range from 10° to 50°, and the minimum is clearly at the angle $\theta = 90°$. Solar irradiation reaches its maximum at 12h30; $\theta = 50°$, $G_{50} = 510$ Wm^2 and its minimum is 390 W/m^2 at 12:00; $\theta = 90°$.

Fig. 24 shows global irradiation as a function of the ratio of the hour angle and the height of the sun (ω/h) according to the tilt angles corresponding to prediction data for a cloudy day. The maximum solar irradiation is in the angle $\theta = 20°$, and the minimum corresponding to $\theta = 90°$. At 11h30 solar irradiation reaches its maximum; $G_{20} = 500$ W/m^2 and its minimum is 380 W/m^2 at 11:30; $\theta = 90°$.

Fig. 25 compares global irradiation according to tilt angles between the proposed model and experimental data on a cloudy day. As is seen from the given graphs the line of the proposed model is close to the experimental data at some points ($\omega/h = 0.58$, 1.4) and a little far at other points ($\omega/h =$ 0.32, –0.56 –1.10).

5. Conclusions

The main purpose of this study is to propose a suitable model for predicting global solar radiation on multiple angles from 0°to 90° in different contexts. The experimental results give perfect global solar irradiation for every month from January to April and for a cloudy day in the Ouled Djellal site of study. We then created a mathematical model to predict the progress of global solar irradiation as a function of the hour angle and the height of the sun. The equation was made more complex by adding the angle of inclination.

We conclude that the experimental data show that global solar irradiation in the tilt angles from 0°to 90° at the site is

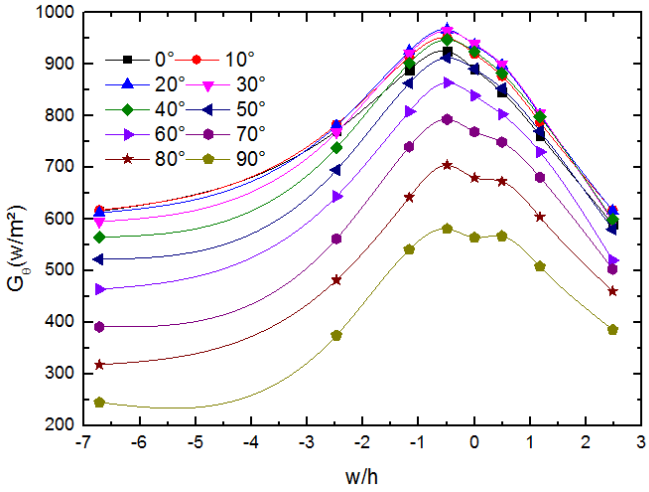

Figure 18: Global irradiation according to tilt angles and ω/h corresponding to experimental data in April

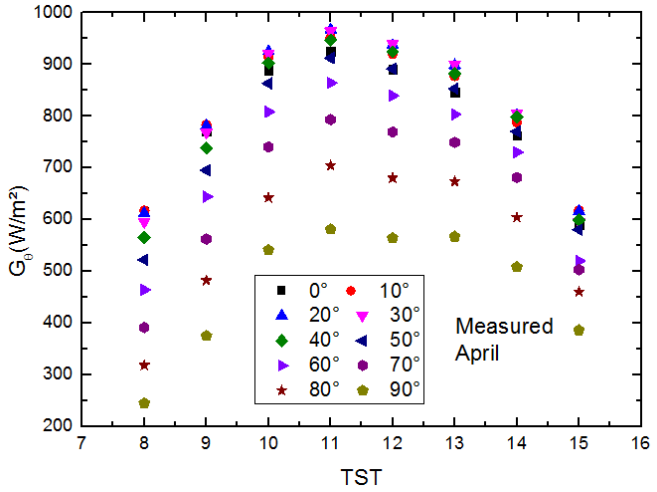

Figure 19: Global irradiation according to tilt angles and TST corresponding to experimental data in April

considerable and the greatest solar irradiation is in the range of 20° to 40°. The comparison of the proposed model with the measured data shows that there is agreement at all the angles which gives us a perfect residual.

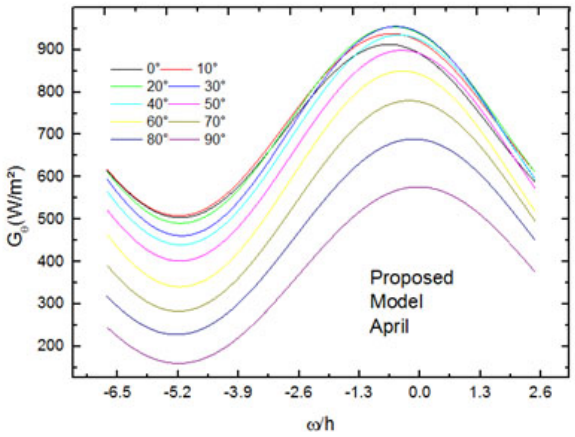

Figure 20: Global irradiation according to tilt angles corresponding to proposed model in April

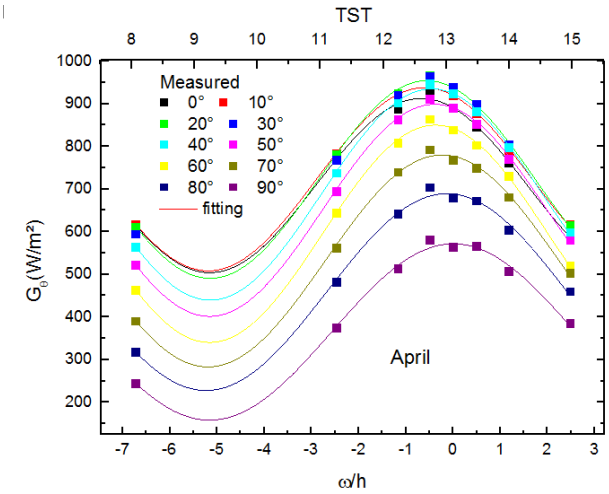

Figure 21: Comparison of global irradiation according to tilt angles between model and experimental data in April

References

[1] C. P. de Brichambaut, C. Vauge, Le gisement solaire: Evaluation de la ressource énergétique, Tec & Doc, 1982.

[2] S. Barbaro, S. Coppolino, C. Leone, E. Sinagra, An atmospheric model for computing direct and diffuse solar radiation, Solar Energy 22 (3) (1979) 225–228.

[3] M. Krarti, J. Huang, D. Seo, J. Dark, Development of solar radiation models for tropical locations, Tech. rep., Draft final report (June 30 2006).

[4] M. Daguenet, Les séchoirs solaires, Unesco, 1985.

[5] A. Dumas, A. Andrisani, M. Bonnici, G. Graditi, G. Leanza, M. Madonia, M. Trancossi, A new correlation between global solar energy radiation and daily temperature variations, Solar Energy 116 (2015) 117–124.

[6] J.-K. Park, A. Das, J.-H. Park, A new approach to estimate the spatial distribution of solar radiation using topographic factor and sunshine duration in south korea, Energy Conversion and Management 101 (2015) 30–39.

[7] R. Benson, M. Paris, J. Sherry, C. Justus, Estimation of daily and monthly direct, diffuse and global solar radiation from sunshine duration measurements, Solar energy 32 (4) (1984) 523–535.

[8] J. Gariepy, Estimation of global solar radiation, International report, Service of Meteorology, Canada (1980).

[9] J. Almorox, C. Hontoria, Global solar radiation estimation using sunshine duration in spain, Energy Conversion and Management 45 (9-10) (2004) 1529–1535.

[10] T. Samuel, Estimation of global radiation for sri lanka, Solar Energy (Journal of Solar Energy Science and Engineering) 47 (5) (1991) 333–337.

[11] M. Trnka, Z. Žalud, J. Eitzinger, M. Dubrovskỳ, Global solar radiation in central european lowlands estimated by various empirical formulae, Agricultural and Forest Meteorology 131 (1-2) (2005) 54–76.

[12] H. C. Power, Estimating clear-sky beam irradiation from sunshine duration, Solar Energy 71 (4) (2001) 217–224.

[13] C. Tiba, Solar radiation in the brazilian northeast, Renewable Energy 22 (4) (2001) 565–578.

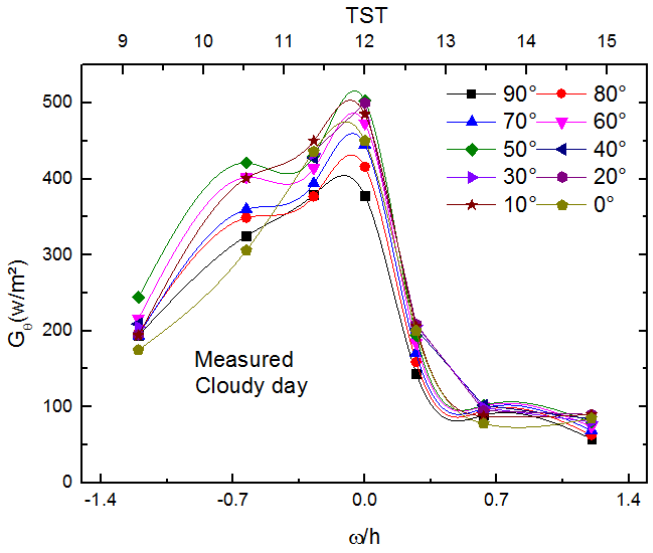

Figure 22: Global irradiation according to tilt angles and ω/h corresponding to experimental data on a cloudy day

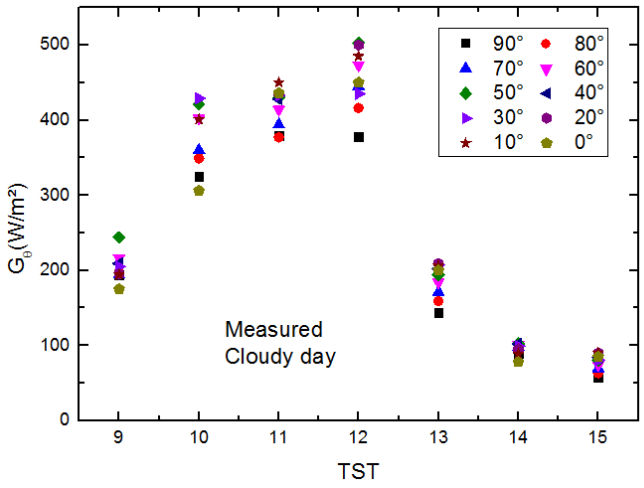

Figure 23: Global irradiation according to tilt angles and TST corresponding to experimental data on a cloudy day

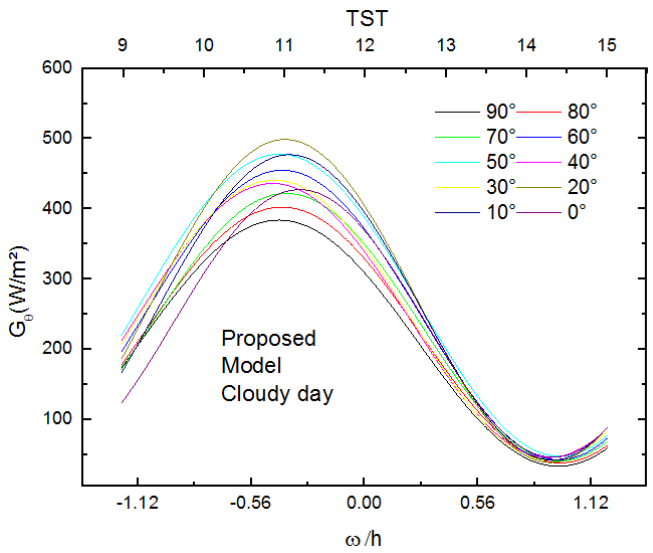

Figure 24: Global irradiation according to tilt angles corresponding to the proposed model for a cloudy day

[14] M.-F. Li, X.-P. Tang, W. Wu, H.-B. Liu, General models for estimating daily global solar radiation for different solar radiation zones in mainland china, Energy conversion and management 70 (2013) 139–148.

[15] A. Katiyar, C. K. Pandey, Simple correlation for estimating the global solar radiation on horizontal surfaces in india, Energy 35 (12) (2010) 5043–5048.

[16] K. Yang, G. Huang, N. Tamai, A hybrid model for estimating global solar radiation, Solar energy 70 (1) (2001) 13–22.

[17] J. K. Yohanna, I. N. Itodo, V. I. Umogbai, A model for determining the global solar radiation for makurdi, nigeria, Renewable Energy 36 (7) (2011) 1989–1992.

[18] D. B. Ampratwum, A. S. Dorvlo, Estimation of solar radiation from the number of sunshine hours, Applied Energy 63 (3) (1999) 161–167.

[19] A. Maghrabi, Parameterization of a simple model to estimate monthly global solar radiation based on meteorological variables, and evaluation of existing solar radiation models for tabouk, saudi arabia, Energy conversion and management 50 (11) (2009) 2754–2760.

[20] J. Almorox, M. Benito, C. Hontoria, Estimation of monthly angström–prescott equation coefficients from measured daily data in toledo, spain, Renewable Energy 30 (6) (2005) 931–936.

[21] H. Duzen, H. Aydin, Sunshine-based estimation of global solar radiation on horizontal surface at lake van region (turkey), Energy Conversion and Management 58 (2012) 35–46.

[22] T. Muneer, M. Gul, Evaluation of sunshine and cloud cover based models for generating solar radiation data, Energy Conversion and Management 41 (5) (2000) 461–482.

[23] F. Chabane, N. Moummi, S. Benramache, Experimental study of heat transfer and thermal performance with longitudinal fins of solar air heater, Journal of advanced research 5 (2) (2014) 183–192.

[24] F. Chabane, N. Moummi, S. Benramache, A. S. Tolba, Experimental study of heat transfer and an effect the tilt angle with variation of the mass flow rates on the solar air heater, Int J Sci Eng Invest 1 (9) (2012) 61–5.

[25] F. Chabane, N. Moummi, S. Benramache, Experimental performance of solar air heater with internal fins inferior an absorber plate: in the region of biskra, Journal of Energy Resources Technology 4 (33) (2012) 1–6.

[26] N. Moummi, F. Chabane, S. Benramache, A. Brima, Thermal efficiency analysis of a single-flow solar air heater with different mass flow rates in a smooth plate, Frontiers in Heat and Mass Transfer (FHMT) 4 (1) (2013) 013006.

[27] F. Chabane, N. Moummi, S. Benramache, D. Bensahal, O. Belahssen, Collector efficiency by single pass of solar air heaters with and without using fins, Engineering journal 17 (3) (2013) 43–55.

[28] F. Chabane, N. Moummi, S. Benramache, Effect of the tilt angle of natural convection in a solar collector with internal longitudinal fins, International Journal of Science and Engineering Investigations 1 (7) (2012) 13–17.

[29] F. Chabane, N. Moummi, S. Benramache, Experimental analysis on thermal performance of a solar air collector with longitudinal fins in a region of biskra, algeria, Journal of Power Technologies 93 (1) (2013) 52–58.

[30] F. Chabane, N. Moummi, S. Benramache, D. Bensahal, O. Belahssan, Nusselt number correlation of SAH, Journal of Power Technologies 93 (2) (2013) 100–110.

[31] F. Chabane, N. Moummi, Heat transfer and energy analysis of a solar air collector with smooth plate, The European Physical Journal-Applied Physics 66 (1) (2014) 10901.

[32] F. Chabane, N. Hatraf, N. Moummi, Experimental study of heat transfer coefficient with rectangular baffle fin of solar air heater, Frontiers in Energy 8 (2) (2014) 160–172.

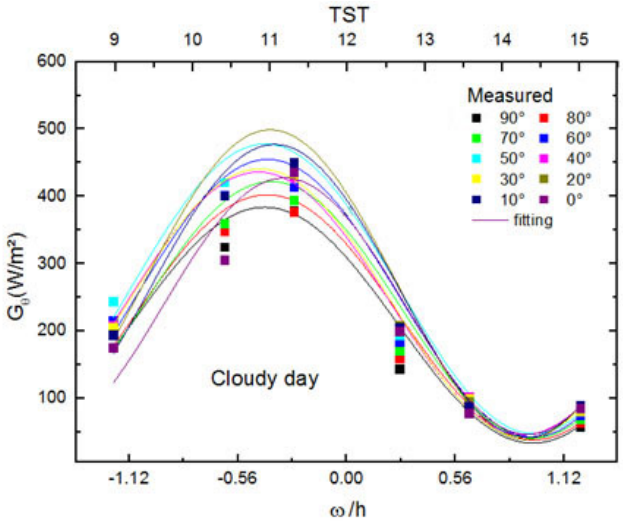

Figure 25: Comparison of global irradiation according to tilt angles between model and experimental data on a cloudy day